Macromolecules
ARTICLE

Macromolecules **2009**, *42*, 7423–7429 **7423**
DOI: 10.1021/ma901100n

Control of Layer Thickness of Onionlike Multilayered Composite Polymer Particles Prepared by the Solvent Evaporation Method†

Takuya Tanaka, Naohiko Saito, and Masayoshi Okubo*

Graduate School of Engineering, Kobe University, Kobe 657-8501, Japan

Received May 20, 2009; Revised Manuscript Received August 19, 2009

ABSTRACT: Micrometer-sized, monodisperse, "onionlike" multilayered polystyrene-*block*-poly(methyl methacrylate) (PS-*b*-PMMA, volume fraction of PS segment in the block copolymer; $f_{PS} \approx 0.5$) particles and PS/PS-*b*-PMMA/PMMA composite particles with different layer thicknesses (D) were successfully prepared by slow release of toluene by evaporation from polymer/toluene droplets dispersed in aqueous media formed using the membrane emulsification method. D is defined as one periodicity consisting of single PS and PMMA layers. The effects of number-average molecular weight (M_n of PS-*b*-PMMA $\approx (7.8-29.0) \times 10^4$ g mol^{-1}) and volume fraction of PS-*b*-PMMA (PS/PS-*b*-PMMA/PMMA = 0/10/0−4.5/1/4.5, v/v/v) on the D of multilayered particles were investigated. The D value increased with an increase in M_n to the 2/3 power, in agreement with theory established in polymer blend film systems. PS ($M_n \approx (1.1-48.9) \times 10^4$ g mol^{-1})/PS-*b*-PMMA ($M_n \approx 29.0 \times 10^4$ g mol^{-1}, $f_{PS} \approx 0.5$)/PMMA ($M_n \approx (1.3-46.9) \times 10^4$ g mol^{-1}) composite particles with various volume fractions were also prepared. When the molecular weights of the homopolymers were lower than those of the corresponding polymer segments in the block copolymer, multilayered structures were observed even at a low volume fraction of the block copolymer. On the other hand, when they were higher, microphase and macrophase-separated structures coexisted in all volume fractions. The D of multilayered particles containing low molecular weight homopolymers was proportional to the −1/3 power of the volume fraction of the block copolymer consistent with the theory of the polymer blend film systems, indicating that the D is controllable by proper selection of the experimental conditions.

Introduction

Morphology of composite polymer particles is directly linked with their physical properties for diverse applications such as impact modifiers, adhesives, and coatings. As a consequence, extensive research has been directed toward morphology control, resulting in the formation of composite polymer particles having a variety of morphologies by various seeded polymerizations.[1−13] Most of work related to morphology control has so far concentrated on macrophase separation between seed polymer and polymer formed in the post-polymerization step as a result of the incompatibility between the polymers.

We have reported a series of considerations dealing with preparation of micrometer-sized, monodisperse, "onionlike" multilayered poly(methyl methacrylate) (PMMA)/polystyrene (PS) composite particles.[14−17] This was first accomplished unexpectedly by restructuring the morphology of PMMA-core/PS-shell particles, which was prepared by seeded dispersion polymerization of styrene in the presence of PMMA seed particles, using the solvent absorbing-releasing method (SARM).[14] Further investigations revealed that PMMA-*graft*-PS and/or PMMA-*block*-PS (PMMA-*b*-PS) formed in PMMA/PS composite particles during the seeded dispersion polymerization acted as compatibilizer in the formation of the microphase-separated multilayered structure (lamellar structure packed into spherical particle) during SARM treatment.[16] Furthermore, we have successfully prepared directly poly(isobutyl methacrylate)-*b*-PS particles with onionlike multilayered structure by two-step atom transfer radical polymerization in an aqueous medium (without post-treatment by organic solvent).[18,19]

In recent years, other groups have also intensively investigated the microphase-separated structure comprising the multiblock copolymer inside the particles (three-dimensional confinement) based on experiment[20−30] and theory.[31,32] In particular, when the ratio of the particle diameter to the equilibrium period of block copolymer was significantly low and not an integer, anomalous microphase-separated structures were developed (confinement effect).[22,24,26,28,29,31,32] Additionally, other approaches for the synthesis of the multilayered particles utilizing sequential seeded polymerization[33−37] and temperature-modulated precipitation polymerization[38] have been reported. Such multilayered particles could be applied to three-dimensional optical memory storage,[34] cavity quantum electrodynamics,[36,37,39] and new photonic devises.[40] From the point of view of these applications, it is of substantial importance to control microphase structures, layer thickness, number of interfaces, and refractive index difference between the polymers for the block copolymer particles.

Over the past three decades, microphase-separated structures in the block copolymer film systems have widely been investigated.[41−54] The covalent bond between dissimilar polymer blocks restricts the macroscopic separation, and this constraint leads to formation of mesoscopic (10 nm scale) self-assembly (lamellar, hexagonal-packed cylinder, bicontinuous cubic gyroid, and body-centered cubic) depending on the polymer compositions in the molten and solid states. In a previous work,[55] we have prepared PS/PS-*b*-PMMA/PMMA particles by slow release of toluene from PS/PS-*b*-PMMA/PMMA/toluene droplets dispersed in an emulsifier aqueous solution using well-defined PS-*b*-PMMA. The morphology of PS/PS-*b*-PMMA/PMMA particles could be controlled from sea−island to cylinder, bicontinuous gyroid, multilayered, and vice versa with each phase inverted by increasing fraction of one polymer phase. Such a microphase transition has also been observed in polymer film systems.

† Part CCCXXIX of the series "Studies on Suspension and Emulsion".

*To whom correspondence should be addressed: Fax +81-78-803-6161; e-mail okubo@kobe-u.ac.jp.

Published on Web 09/01/2009

Table 1. Molecular Weights of PS-*b*-PMMA[a], PS, and PMMA

polymer	M_n^{PS} ($\times 10^4$ g mol^{-1})[d]	M_n^{PMMA} ($\times 10^4$ g mol^{-1})[e]	PDI[f]	f_{PS}[g]
PS-*b*-PMMA8	3.65	4.15	1.06	0.50
PS-*b*-PMMA20	9.20	10.80	1.09	0.49
PS-*b*-PMMA26	12.20	14.10	1.15	0.49
PS-*b*-PMMA29	12.95	16.05	1.16	0.48
PS1[b]	1.06		1.10	
PMMA1[b]		1.33	1.09	
PS49[c]	48.94		1.95	
PMMA47[c]		46.93	2.18	

[a] Purchased from Polymer Source Inc. [b] Prepared by bulk ATRP. [c] Prepared by bulk polymerization. [d] Number-average molecular weights of PS and PS block in PS-*b*-PMMA. [e] Number-average molecular weights of PMMA and PMMA block in PS-*b*-PMMA. [f] Polydispersity index. [g] Volume fraction of PS block in PS-*b*-PMMA.

On the basis of this finding, the theory of microphase separation of polymer blend film systems might be applicable to polymer colloid systems.

In the present study, we focused on the control of the layer thickness (D) of the onionlike multilayered particles prepared by slow release of toluene from PS-*b*-PMMA/toluene and PS/PS-*b*-PMMA/PMMA/toluene droplets dispersed in 0.5 wt % sodium dodecyl sulfate (SDS) aqueous solution as functions of number-average molecular weight (M_n) and volume fraction ($\phi_{PS\text{-}b\text{-}PMMA}$) of the block copolymer.

Experimental Section

Materials. Styrene and methyl methacrylate (MMA) were distilled under reduced pressure in a nitrogen atmosphere. Ethyl 2-bromoisobutyrate (EB*i*B) (Tokyo Kasei Kogyo Co. Ltd., Tokyo, Japan), *N,N,N′,N′,N″*-pentamethyldiethylenetriamine (PMDETA), 4,4′-dinonyl-2,2′-dipyridyl (dNdpy) (Aldrich Chemical Co. Ltd.), and CuBr (Nacalai Tesque Inc., Kyoto, Japan) were used as received. PS-*b*-PMMA purchased from Polymer Source Inc. (Canada) was used as received. Deionized water was used after distillation. SDS and toluene were used as received from Nacalai Tesque Inc., Japan.

Preparation of PS and PMMA. PS and PMMA with low molecular weight were prepared by atom transfer radical polymerization in bulk (bulk ATRP) as follows: Homogeneous solutions of styrene/EB*i*B/CuBr/PMDETA (200/1/1/1, mol/mol/mol/mol) and MMA/EB*i*B/CuBr/dNbpy (200/1/1/2, mol/mol/mol/mol) were added into glass tubes, sealed off under a nitrogen atmosphere. The polymerizations of styrene and MMA were carried out at 70 °C for 8 h and at 40 °C for 1.5 h, respectively. The glass tubes were shaken horizontally at a rate of 100 cycles/min in a water bath.

PS and PMMA with high molecular weight were prepared by bulk polymerization using AIBN as an initiator (0.010 wt % vs styrene and 2.0 wt % vs MMA). Homogeneous solutions of the monomer (styrene or MMA) and AIBN were transferred to glass tubes, degassed with nitrogen several times, and subsequently sealed off under vacuum. The polymerizations of styrene and MMA were carried out at 50 °C for 48 h and 30 °C for 6 h, respectively. The glass tubes were shaken as shown above. The products were precipitated in methanol to remove the residual monomer and subsequently dried under vacuum at room temperature. The molecular weights and the molecular weight distributions of the polymers are listed in Table 1.

Preparation of Composite Polymer Particles. The mixture (10 g) of PS, PMMA, PS-*b*-PMMA, and toluene (polymer/toluene = 1/10 or 1/100, w/w) was stored in a Teflon storage tank and permeated through a microporous glass membrane (SPG Technology Co., Ltd., Japan) with an average pore size of 1.3 μm membrane into 0.5 wt % SDS aqueous solution under an appropriate pressure (ca. 0.03 MPa). Toluene was slowly released by evaporation from the dispersion under gentle stirring with a magnetic stirrer at room temperature for 24 h in an uncovered beaker. Polymer particles were collected by centrifugation, washed with methanol for several times to remove excess SDS, and subsequently dried under vacuum at room temperature.

Preparation of Polymer Blend Films. A homogeneous toluene solution of PS, PMMA, and PS-*b*-PMMA (polymer/toluene = 1/10 or 1/30, w/w) was cast into a mold (2.25 cm^2 surface area between solution and air). Toluene was slowly evaporated from the solution at room temperature for 24 h. Polymer films were dried under vacuum at room temperature. The film thicknesses were ~200 μm in all cases.

Measurements. The amount of toluene in the dispersion was determined by gas chromatography (Shimadzu Corp., GC-2014) with helium as the carrier gas, *N,N*-dimethylformamide as a solvent, and *p*-xylene as an internal standard. Molecular weight distributions were measured by gel permeation chromatography (GPC) with two S/DVB gel columns (TOSOH Corp., TSK gel GMH$_{HR}$-H, 7.8 mm i.d. × 30 cm) using tetrahydrofuran as eluent at 40 °C at flow rate of 1.0 mL min^{-1} employing refractive index (TOSOH RI-8020/21) and ultraviolet detectors (TOYO SODA UV-8II). The columns were calibrated with six standard PS samples (1.05×10^3−5.48×10^6, M_w/M_n = 1.01−1.15). The volume fractions of PS and PMMA blocks in PS-*b*-PMMA were measured by ^{1}H NMR with a Bruker DPX 250 MHz spectrometer (Karlsruhe, Germany).

Observation of Composite Polymer Particles. PS-*b*-PMMA particles and PS/PS-*b*-PMMA/PMMA composite particles were observed with a MICROPHOT-FXA optical microscope and a Hitachi S-2460 scanning electron microscope (SEM) at an acceleration voltage of 15 kV. The dried particles were stained with ruthenium tetraoxide (RuO_4) vapor at room temperature for 30 min in the presence of 1% RuO_4 aqueous solution, embedded in an epoxy matrix, cured at room temperature, and subsequently microtomed. Ultrathin cross sections of 100 nm thickness were observed with a JEOL JEM-1230 transmission electron microscope (TEM) at an acceleration voltage of 100 kV. The diameter values of 100 particles in TEM photograph (not cross-sectional image) were measured to evaluate number-average diameters (d_n) and its coefficient of variations (C_v) using image analysis software for a Macintosh computer (MacSCOPE, Mitani Co. Ltd.).

Results and Discussion

Effect of Molecular Weight of PS-*b*-PMMA. Figure 1 shows SEM photographs of PS-*b*-PMMA particles with various M_n obtained by slow release of toluene from PS-*b*-PMMA/toluene (1/100, w/w) droplets dispersed in 0.5 wt % SDS aqueous solution. The monodisperse PS-*b*-PMMA/toluene droplets having d_n of ca. 6.5 μm were prepared by permeation of polymer solution through the Shirasu porous glass (SPG) membrane into the SDS aqueous solution. The amounts of residual toluene after 24 h evaporation from the dispersions measured by gas chromatography were less than 1 wt % of the initial amounts. Monodisperse spherical particles were obtained without coagulation during toluene evaporation. The d_n and C_v of the particles were approximately 1.4 μm and 10%, respectively, in all cases. The final particle sizes were consistent with expectation based on the droplet sizes and the polymer concentration.

Figure 2 shows TEM photographs of ultrathin cross sections of RuO_4-stained PS-*b*-PMMA particles with the various M_n. RuO_4 stains PS but not PMMA.[56] "Onionlike" multilayered structures were observed in all cases. The D of the multilayered structure, which is defined as one periodicity consisting of single PS and PMMA layers, increased with increasing M_n. The PS layer seemed to be thicker than the PMMA layer in the particles even though the volume fraction of PS block (f_{PS}) in PS-*b*-PMMA was ~0.5. This might

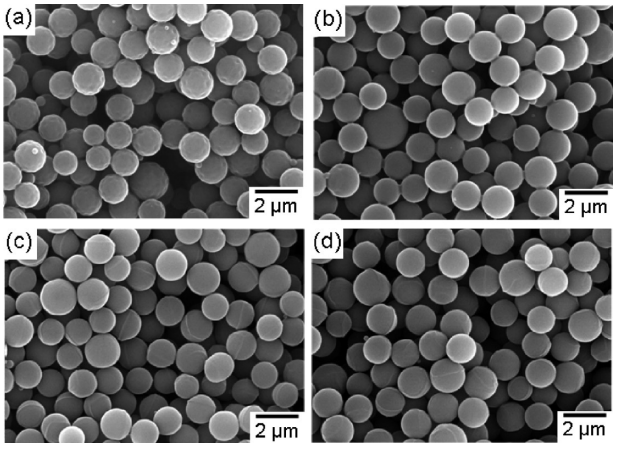

Figure 1. SEM photographs of PS-*b*-PMMA particles obtained by slow release of toluene from PS-*b*-PMMA/toluene (1/100, w/w) droplets dispersed in 0.5 wt % SDS aqueous solution, which were prepared by the SPG method. M_n of PS-*b*-PMMA ($\times 10^4$ g mol^{-1}): (a) 7.8; (b) 20.0; (c) 26.3; (d) 29.0. f_{PS}: (a) 0.50; (b) 0.49; (c) 0.49; (d) 0.48.

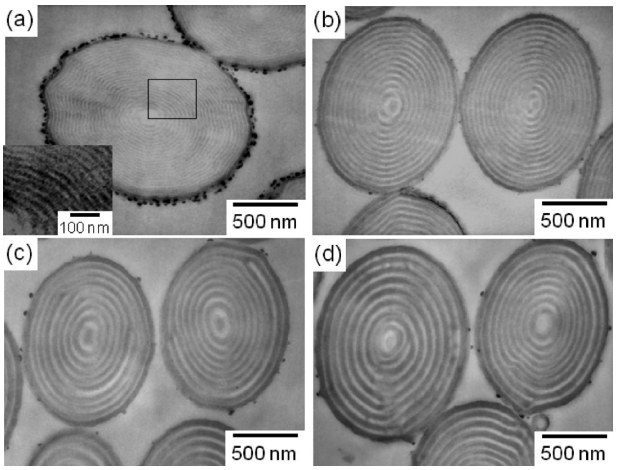

Figure 2. TEM photographs of ultrathin cross sections of RuO_4-stained PS-*b*-PMMA particles obtained by slow release of toluene from PS-*b*-PMMA/toluene (1/100, w/w) droplets dispersed in 0.5 wt % SDS aqueous solution, which were prepared by the SPG method. M_n of PS-*b*-PMMA ($\times 10^4$ g mol^{-1}): (a) 7.8; (b) 20.0; (c) 26.3; (d) 29.0. f_{PS}: (a) 0.50; (b) 0.49; (c) 0.49; (d) 0.48. PS and PMMA layers appear as dark and bright rings, respectively. The outermost layer of PMMA is not shown due to low electron contrast between PMMA layers and the epoxy resin matrix.

be due to the cutting position of the ultrathin cross section and RuO_4 staining not only pure PS layer but also the interface between the PS and PMMA layers. Moreover, the outermost layer was occupied by PMMA, which was confirmed by X-ray photoelectron spectroscopy, because the interfacial tension between PMMA and the aqueous medium was lower than that between PS and the aqueous medium when SDS was employed as an emulsifier.[57] On the other hand, the polymer phase of the innermost layer; that is, the core could be either PS or PMMA. The polymer phase of the core and its diameter were determined by the ratio of the particle diameter to the layer thickness of the multilayered particles because the multilayered structure formed from the outermost layer.[55] In other words, it is possible to tune the polymer phase of the core and its diameter if the particle diameter can precisely be controlled in hundreds of nanometers.

When the volume fractions of PS and PMMA blocks in the PS-*b*-PMMA are similar, self-assembled PS and PMMA blocks develop microphase separation resulting in the formation of flat interfaces (lamellar structure) in films. On the other hand, they pack along curved interfaces due to the spatial restriction in the spherical particles. The interior block should stretch up toward the center of the particles more than the exterior block to keep the densities of the blocks constant. The conformation of the block copolymer oriented in the spherical particles is thus affected by the curvature to some degree. On the basis of this consideration, the layer thickness of the multilayered particles should be slightly thicker than that of the polymer lamellar film. Yu et al. systematically examined the self-assembled morphology for symmetric diblock copolymers confined in spherical pores using Monte Carlo simulations.[32] Their prediction indicated that the repeat period for the concentric-spherical lamellar (onionlike multilayered structure) was slightly larger than that for the bulk lamellar.

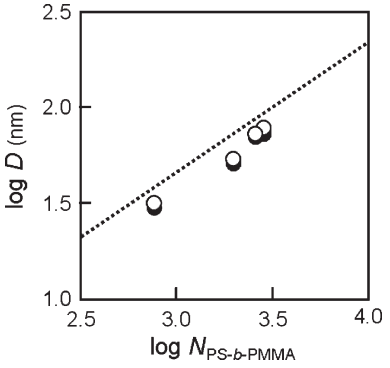

Figure 3. Relationship between degree of polymerization of PS-*b*-PMMA ($N_{PS\text{-}b\text{-}PMMA}$) and the layer thicknesses (D) of the multilayered structures of PS-*b*-PMMA in the particles (○) estimated from Figure 2 and in the films (●) cast from toluene solutions (see Figure S1). Dotted line and circles show theoretical and experimental values, respectively.

The D values of the multilayered particles were estimated from TEM photographs of ultrathin cross sections by the length of layers (excluding the core) divided by the number of layers. Only ultrathin cross sections having the average particle diameter, which means that the sections were cut from the center of the particles, for at least 20 sections were used for the measurement to reduce experimental errors. The molecular weight dependence of the D of lamellar morphology of polymer blend films has been extensively investigated.[58−61] These studies are represented by a N^z dependence on molecular weight, where N is degree of polymerization of the block copolymer, and the scaling exponent z was estimated to be 2/3 or very close to 2/3. In the present study, the following equation developed by Semenov[59] was used for the calculation of D of the lamellar morphology in the strong segregation limit.

$$D \cong 1.098 N^{2/3} a \chi^{1/6} \tag{1}$$

where a is a statistical segment length and χ is a Flory−Huggins interaction parameter. The temperature dependence of $\chi_{PS/PMMA}$ is expressed as[62]

$$\chi_{PS/PMMA} = 0.0284 + \frac{3.902}{T} \tag{2}$$

We used $\chi_{PS/PMMA} = 0.0414$ ($T = 300$ K) and $a = 0.71$ nm (average value of $a_{PS} = 0.67$ nm and $a_{PMMA} = 0.75$ nm)[63] for the calculation of the theoretical D of the lamellar morphology.

Figure 3 shows the relationship between the degree of polymerization of PS-*b*-PMMA ($N_{PS\text{-}b\text{-}PMMA}$) and the

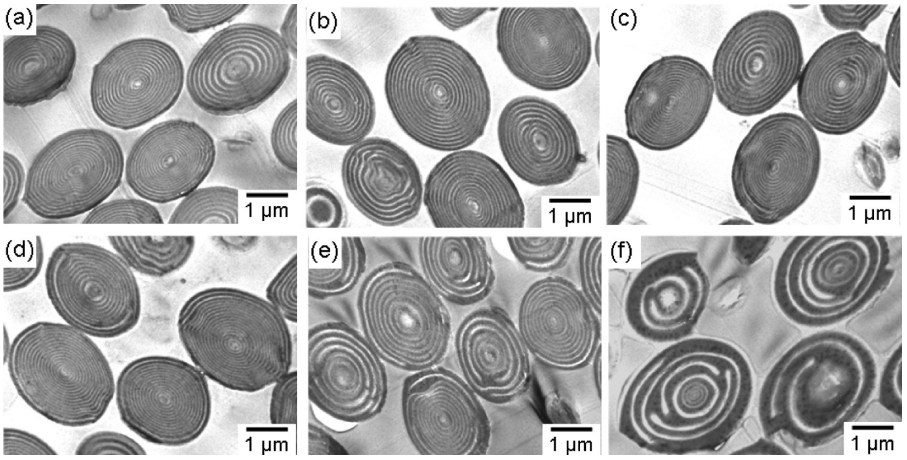

Figure 4. TEM photographs of ultrathin cross sections of RuO_4-stained PS1/PS-*b*-PMMA29/PMMA1 composite particles obtained by slow release of toluene from the polymer/toluene (1/10, w/w) droplets dispersed in 0.5 wt % SDS aqueous solution, which were prepared by the SPG method. $\phi_{PS}/\phi_{PS\text{-}b\text{-}PMMA}/\phi_{PMMA}$: (a) 0/1/0; (b) 0.1/0.8/0.1; (c) 0.2/0.6/0.2; (d) 0.3/0.4/0.3; (e) 0.4/0.2/0.4; (f) 0.45/0.1/0.45. M_n (g mol^{-1}) of PS1, PMMA1, and PS-*b*-PMMA29 were respectively 1.06×10^4, 1.33×10^4, and 29.0×10^4. PS and PMMA layers appear as dark and bright rings, respectively. The outermost layer of PMMA is not shown due to low electron contrast between PMMA layers and the epoxy resin matrix.

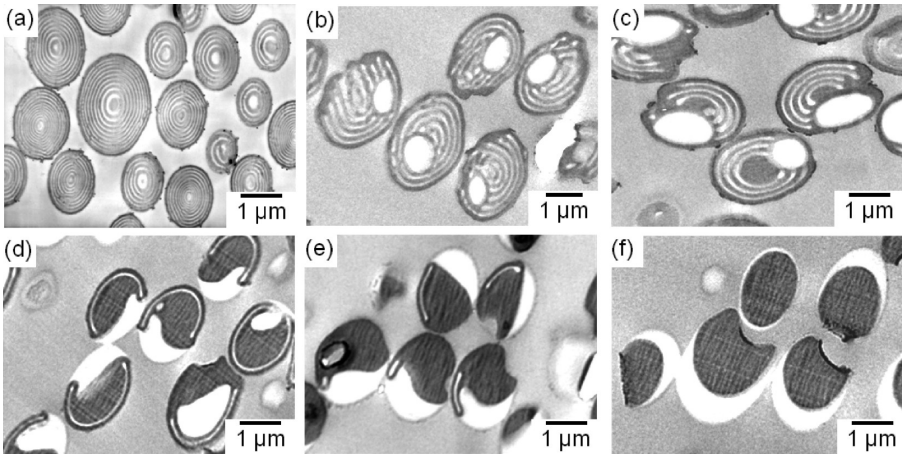

Figure 5. TEM photographs of ultrathin cross sections of RuO_4-stained PS49/PS-*b*-PMMA29/PMMA47 composite particles obtained by slow release of toluene from the polymer/toluene (1/100, w/w) droplets dispersed in 0.5 wt % SDS aqueous solution, which were prepared by the SPG method. $\phi_{PS}/\phi_{PS\text{-}b\text{-}PMMA}/\phi_{PMMA}$: (a) 0/0.1/0; (b) 0.1/0.8/0.1; (c) 0.2/0.6/0.2; (d) 0.3/0.4/0.3; (e) 0.4/0.2/0.4; (f) 0.45/0.1/0.45. M_n (g mol^{-1}) of PS49 and PMMA47 were respectively 48.9×10^4 and 46.9×10^4. PS and PMMA layers appear as dark and bright rings, respectively. The outermost layer of PMMA is not shown due to low electron contrast between PMMA layers and the epoxy resin matrix.

experimental D values of the multilayered structure in the particles estimated from Figure 2 and in the films (see Figure S1) cast from toluene solutions. The experimental D values of the particles (open circles) were almost the same as that of the films (closed circles); that is, the effect of curvature (three-dimensional confinement) on the layer thickness of the multilayered morphology was not observed. In the current study, the particle diameter was significantly larger than the layer thickness. Thus, the confinement effect on the layer thickness might be weak because the confinement effect can be pronounced with decreasing the ratio of the diameter to the equilibrium period of block copolymer.[64,65] Additionally, the experimental D of the multilayered particles, which were 31.7, 52.6, 71.4, and 76.9 nm in ascending order, increased with increasing $N_{PS\text{-}b\text{-}PMMA}$ to the 2/3 power consistent with the theory. However, the experimental D values of the particles (and the films) with various $N_{PS\text{-}b\text{-}PMMA}$ were somewhat lower than predicted D values (dotted line) as shown in Figure 3. The layer thickness of the multilayered structure consisting of PS-*b*-PMMA might be kinetically controlled at the final stage of the toluene evaporation because of significantly lower mobility of the PS-*b*-PMMA chain at room temperature. Consequently, the polymer chains could not stretch to the same extent as thermodynamic equilibrium morphology.[66]

Effect of Volume Fraction of PS-*b*-PMMA. Figure 4 shows TEM photographs of ultrathin cross sections of the PS1/PS-*b*-PMMA29/PMMA1 (see Table 1) composite particles with various volume fractions of block copolymer ($\phi_{PS\text{-}b\text{-}PMMA}$) with keeping the same volume of the PS and PMMA phases. M_n values of PS and PMMA were much lower than those of corresponding blocks of the PS-*b*-PMMA. The d_n and C_v of the particles were approximately 3.0 μm and 10%, respectively, in all cases. The multilayered structure was observed even at a low $\phi_{PS\text{-}b\text{-}PMMA}$ in the particles, and the D increased with a decrease in the $\phi_{PS\text{-}b\text{-}PMMA}$. These results were the same tendency as PS1/PS-*b*-PMMA29/PMMA1 blend films cast from toluene solutions (see Figure S2).

Figure 5 shows TEM photographs of ultrathin cross sections of PS49/PS-*b*-PMMA29/PMMA47 composite particles with various $\phi_{PS\text{-}b\text{-}PMMA}$. M_n values of PS and PMMA were much higher than those of corresponding blocks of the

PS-*b*-PMMA. The "onionlike" multilayered structure was not observed, and microphase (multilayered) and macrophase (PMMA and/or PS domains) separated structures coexisted inside the particles. With decreasing $\phi_{PS\text{-}b\text{-}PMMA}$, macrophase separation became dominant. On the other hand, in the PS49/PS-*b*-PMMA29/PMMA47 blend films cast from toluene solutions, microphase (lamellar and/or ellipsoidal multilayered) and macrophase (PMMA domains) separated structures coexisted even at a low $\phi_{PS\text{-}b\text{-}PMMA}$ (see Figure S3). This morphological difference between the particles and the films might be due to the total interfacial area between PS and PMMA homopolymer phases where the block copolymer located. PS49/PS-*b*-PMMA29/PMMA47 composite particles containing below 20 vol % block copolymer had a single dimple at the surface (Figure 5e,f; see also Figure S4). As described in our previous study,[67] PS/PMMA (without PS-*b*-PMMA) composite particles with macrophase-separated structure had a single dimple at the surface as a result of the volume reduction of the PS phase after hardening of the PMMA phase during toluene releasing from the corresponding droplets. This might explain the reason that the PS49/PS-*b*-PMMA29/PMMA47 composite particles had a single dimple at the surface. This nonspherical shape would not affect the phase separated structure inside the particle because the particle deformation occurred at the final stage of the toluene evaporation where the phase-separated structure had already been determined.

The phase transition for the ternary mixtures of block copolymer and corresponding homopolymers in polymer film systems has been extensively investigated.[68−78] To understand the molecular weight dependence of the phase transition in the current study, phase diagrams were constructed on the basis of the theory in the polymer film systems reported by Hashimoto and co-workers.[72] Figure 6 shows phase diagrams indicating the stability limits for the microphase and macrophase transitions for the ternary mixture of PS/PS-*b*-PMMA/PMMA. The parameters using for the calculation were as follows: $f_{PS} = 0.48$, $\phi_{PS} = \phi_{PMMA} = (1 - \phi_{PS\text{-}b\text{-}PMMA})/2$ and $N_{PS\text{-}b\text{-}PMMA} = 2850$. In the calculation, the same average values are used for $N_{PS}/N_{PS\text{-}b\text{-}PMMA}$ and $N_{PMMA}/N_{PS\text{-}b\text{-}PMMA}$, 0.041 or 1.65, which are respectively obtained as average values of 0.036 and 0.047 or 1.65 and 1.65 (see Table 1), where N_{PS} and N_{PMMA} are respectively the degree of polymerization of PS and PMMA. Below the stability limit lines of the microphase and macrophase transitions, the systems are in the disordered state. As toluene evaporates, the interaction parameter $\chi_{PS\text{-}b\text{-}PMMA}$ increases,[79] and $(\chi N)_{PS\text{-}b\text{-}PMMA}$ crosses the stability limit line; eventually, microphase or macrophase separation occurs. In the case of PS1/PS-*b*-PMMA29/PMMA1 (Figure 6a), microphase separation dominates, whereas macrophase separation dominates in the case of PS49/PS-*b*-PMMA29/PMMA47 (Figure 6b). These findings are in close agreement with the results from the particle morphologies as shown in Figures 4 and 5. The reason for the coexistence of microphase and macrophase-separated morphologies in the case of PS49/PS-*b*-PMMA29/PMMA47 might be related to the slightly broad molecular weight distribution of the homopolymers. The differences in the phase transition between PS1/PS-*b*-PMMA29/PMMA1 and PS49/PS-*b*-PMMA29/PMMA47 would be attributed to the location of the homopolymers in the polymer blends.

The location of homopolymers in block copolymer phase depends on the ratios of molecular weights of the homopolymers to those of corresponding segments in the block copolymer.[75] When the molecular weights of the homopolymers are lower than those of the corresponding segments in the block copolymer, the homopolymers are solubilized in the block copolymer phase. However, when the molecular weights of the homopolymers are higher than those of the corresponding segments in block copolymer, the homopolymers are segregated from the block copolymer phase. From the viewpoint of the volumetric considerations, the expansion of D by the addition of the homopolymers is intimately related to the change of the interfacial density of the chemical junctions of the block copolymer. As a consequence, when homopolymers are segregated from block copolymer layers assuming no change of the interfacial density of the chemical junctions, the D is expressed as

$$D = D_0/\phi_b \tag{3}$$

where D_0 is D before addition of homopolymers and ϕ_b is volume fraction of block copolymer. On the other hand, when homopolymers are solubilized in block copolymer layers, the D is expressed as

$$D = D_0/\phi_b^{1/3} \tag{4}$$

When solubilizing the homopolymer into block copolymer layers uniformly, chemical junctions of block copolymer would be expanded allowing the $-1/3$ power law of ϕ_b in the polymer film systems.[75] In the present study, when high molecular weight homopolymers were employed, multilayered structure was not observed.

Figure 7 shows the relationship between $\phi_{PS\text{-}b\text{-}PMMA}$ and D of the multilayered structure of PS1/PS-*b*-PMMA29/PMMA1 in the particles and the films obtained from the TEM photographs (Figure 4 and Figure S2). The experimental D of the multilayered particles, which were 76.9, 82.4,

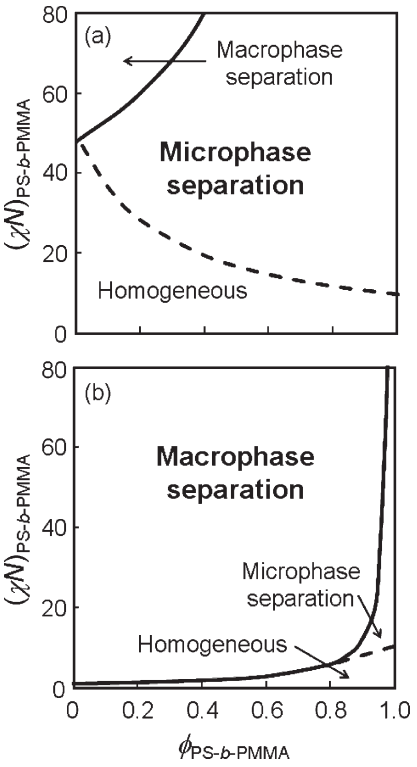

Figure 6. Phase diagrams for the spinodal points for the microphase (broken line) and macrophase (solid line) transition plotted as a function of $\phi_{PS\text{-}b\text{-}PMMA}$ for the ternary mixture of PS/PS-*b*-PMMA/PMMA. $f_{PS} = 0.48$, $\phi_{PS} = \phi_{PMMA} = (1 - \phi_{PS\text{-}b\text{-}PMMA})/2$, $N_{PS\text{-}b\text{-}PMMA} = 2850$, $N_{PS}/N_{PS\text{-}b\text{-}PMMA} = N_{PMMA}/N_{PS\text{-}b\text{-}PMMA} = 0.041$ (a) or 1.65 (b).

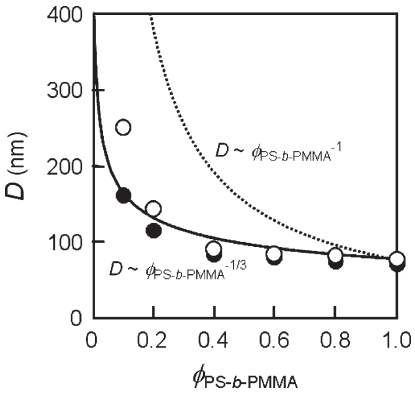

Figure 7. Relationship between volume fraction of PS-*b*-PMMA ($\phi_{PS\text{-}b\text{-}PMMA}$) and the layer thickness (D) of the multilayered structures of PS1/PS-*b*-PMMA29/PMMA1 in the particles (○) estimated from Figure 4 and in the blend films (●) cast from toluene solutions (see Figure S2). Open and closed circles denote the experimental values. Dotted and solid lines show the calculated values when homopolymers are segregated from ($D \sim \phi_{PS\text{-}b\text{-}PMMA}^{-1}$) and solubilized in ($D \sim \phi_{PS\text{-}b\text{-}PMMA}^{-1/3}$) block copolymer layers,[75] respectively.

83.3, 90.9, 142.8, and 250.0 nm in ascending order, were proportional to the $-1/3$ power of $\phi_{PS\text{-}b\text{-}PMMA}$ consistent with theory despite some deviations. Thus, the homopolymers would be solubilized uniformly into the multilayered structure due to their low molecular weights. Additionally, the experimental D values of the particles were similar to those of the blend films except the case of 10 vol % block copolymer.

From the above results, it is concluded that the layer thickness of multilayered particles comprising block copolymer and corresponding homopolymers can be increased by an increase in the molecular weight and a decrease in the volume fraction of block copolymer. Regularly arranged multilayered structures develop the structural color depending on the structural period as a result of interference of light.[80,81] These results suggest that the control of the layer thickness of the multilayered structure might create the polymer particles exhibiting novel optical properties.

Conclusions

Micrometer-sized, monodisperse, "onionlike" multilayered PS-*b*-PMMA particles and PS/PS-*b*-PMMA/PMMA composite particles were prepared by slow release of toluene from polymer/toluene droplets, which were prepared using the SPG method, dispersed in 0.5 wt % SDS aqueous solution. The layer thickness of multilayered PS-*b*-PMMA particles increased with an increase in molecular weight ($M_n \approx (7.8-29.0) \times 10^4$ g mol^{-1}). Quantitative analyses of the TEM observation indicate that the experimental layer thickness of the multilayered structure in the particles varied with the total molecular weight to the 2/3 power in agreement with theory. Moreover, the layer thickness of PS ($M_n \approx 1.1 \times 10^4$ g mol^{-1})/PS-*b*-PMMA ($M_n \approx 29.0 \times 10^4$ g mol^{-1})/PMMA ($M_n \approx 1.3 \times 10^4$ g mol^{-1}) (equal volume fractions of PS and PMMA blocks) composite particles was proportional to the $-1/3$ power of the volume fraction of block copolymers, consistent with theory. In other words, the homopolymers are solubilized uniformly in the corresponding phases of the block copolymer, and thus the multilayered structure is preserved down to a low level of volume fraction of PS-*b*-PMMA. On the basis of these results, it is concluded that the layer thickness of multilayered particles can thus be controlled by proper selection of the molecular weight and the volume fraction of block copolymer.

Acknowledgment. This work was supported by Creation and Support program for Start-ups from Universities (No. 1509) from the Japan Science and Technology Agency (JST) and by Research Fellowships of the Japan Society for the Promotion of Science (JSPS) for Young Scientists (given to N.S.).

Supporting Information Available: TEM photographs of ultrathin cross sections of PS-*b*-PMMA and PS/PS-*b*-PMMA/PMMA blend films and SEM photographs of PS/PS-*b*-PMMA/PMMA composite particles. This material is available free of charge via the Internet at http://pubs.acs.org.

References and Notes

(1) Okubo, M.; Katsuta, Y.; Matsumoto, T. *J. Polym. Sci., Polym. Lett. Ed.* **1980**, *18*, 481–486.
(2) Okubo, M.; Yamada, A.; Matsumoto, T. *J. Polym. Sci., Polym. Chem. Ed.* **1980**, *16*, 3219–3228.
(3) Okubo, M.; Katsuta, Y.; Matsumoto, T. *J. Polym. Sci., Polym. Lett. Ed.* **1982**, *20*, 45–51.
(4) Min, T. I.; Klein, A.; El-Aasser, M. S.; Vanderhoff, J. W. *J. Polym. Sci., Polym. Lett. Ed.* **1983**, *21*, 2845–2861.
(5) Dimonie, V.; El-Aasser, M. S.; Klein, A.; Vanderhoff, J. W. *J. Polym. Sci., Polym. Chem. Ed.* **1984**, *22*, 2197–2215.
(6) Cho, I.; Lee, K.-W. *J. Appl. Polym. Sci.* **1985**, *30*, 1903–1926.
(7) Okubo, M. *Makromol. Chem., Macromol. Symp.* **1990**, *35/36*, 307–325.
(8) Sheu, H. R.; El-Aasser, M. S.; Vanderhoff, J. W. *J. Polym. Sci., Part A: Polym. Chem.* **1990**, *28*, 629–651.
(9) Sundberg, D. C.; Casassa, A. P.; Pantazopoulos, J.; Muscato, M. R. *J. Appl. Polym. Sci.* **1990**, *41*, 1425–1442.
(10) Winzor, C. L.; Sundberg, D. C. *Polymer* **1992**, *33*, 3797–3810.
(11) Dimonie, V. L.; Daniels, E. S.; Shaffer, O. L.; El-Aasser, M. S. In *Emulsion Polymerization and Emulsion Polymers*; Lovell, P. A., El-Aasser, M. S., Eds.; John Wiley & Sons: New York, 1997; Chapter 9, p 293.
(12) Tauer, K.; Riedelsberger, K.; Deckwer, R.; Zimmermann, A. *Macromol. Symp.* **2000**, *155*, 95–104.
(13) Sundberg, D. C.; Durant, Y. G. *Polym. React. Eng.* **2003**, *11*, 379–432.
(14) Okubo, M.; Izumi, J.; Takekoh, R. *Colloid Polym. Sci.* **1999**, *277*, 875–880.
(15) Okubo, M.; Takekoh, R.; Izumi, J. *Colloid Polym. Sci.* **2001**, *279*, 513–518.
(16) Okubo, M.; Takekoh, R.; Saito, N. *Colloid Polym. Sci.* **2003**, *281*, 945–950.
(17) Okubo, M.; Takekoh, R.; Saito, N. *Colloid Polym. Sci.* **2004**, *282*, 1192–1197.
(18) Kagawa, Y.; Minami, H.; Okubo, M.; Zhou, J. *Polymer* **2005**, *46*, 1045–1049.
(19) Kitayama, Y.; Yorizane, M.; Kagawa, Y.; Minami, H.; Zetterlund, P. B.; Okubo, M. *Polymer* **2009**, *50*, 3182–3187.
(20) Lu, Z.; Liu, G.; Phillips, H.; Hill, J. M.; Chang, J.; Kydd, R. A. *Nano Lett.* **2001**, *1*, 683–687.
(21) Takekoh, R.; Okubo, M.; Araki, T.; Stöver, H. D. H.; Hitchcock, A. P. *Macromolecules* **2005**, *38*, 542–551.
(22) Arsenault, A. C.; Rider, D. A.; Tétreault, N.; Chen, J. I. L.; Coombs, N.; Ozin, G. A.; Manners, I. *J. Am. Chem. Soc.* **2005**, *127*, 9954–9955.
(23) Yabu, H.; Higuchi, T.; Shimomura, M. *Adv. Mater.* **2005**, *17*, 2062–2065.
(24) Jeon, S.-J.; Yi, G.-R.; Koo, C. M.; Yang, S.-M. *Macromolecules* **2007**, *40*, 8430–8439.
(25) Charleux, B.; Nicolas, J. *Polymer* **2007**, *48*, 5813–5833.
(26) Rider, D. A.; Chen, J. I. L.; Eloi, J.-C.; Arsenault, A. C.; Russel, T. P.; Ozin, G. A.; Manners, I. *Macromolecules* **2008**, *41*, 2250–2259.
(27) Hales, K.; Chen, Z.; Wooley, K. L.; Pochan, D. J. *Nano Lett.* **2008**, *8*, 2023–2026.
(28) Jeon, S.-J.; Yi, G.-R.; Yang, S.-M. *Adv. Mater.* **2008**, *20*, 1–6.
(29) Higuchi, T.; Tajima, A.; Motoyoshi, K.; Yabu, H.; Shimomura, M. *Angew. Chem., Int. Ed.* **2008**, *47*, 8044–8046.
(30) Higuchi, T.; Tajima, A.; Motoyoshi, K.; Yabu, H.; Shimomura, M. *Angew. Chem., Int. Ed.* **2009**, *48*, 5125–5128.
(31) He, X.; Song, M.; Liang, H.; Pan, C. *J. Chem. Phys.* **2001**, *114*, 10510–10513.
(32) Yu, B.; Li, B.; Jin, Q.; Ding, D.; Shi, A.-C. *Macromolecules* **2007**, *40*, 9133–9142.

(33) Okubo, M.; Takekoh, R.; Sugano, H. *Colloid Polym. Sci.* **2000**, *278*, 559–564.
(34) Pham, H. H.; Gourevich, I.; Oh, J. K.; Jonkman, J. E. N.; Kumacheva, E. *Adv. Mater.* **2004**, *16*, 516–520.
(35) Gourevich, I.; Field, L. M.; Wei, Z.; Paquet, C.; Petukhova, A.; Alteheld, A.; Kumacheva, E.; Saarinen, J. J.; Sipe, J. E. *Macromolecules* **2006**, *39*, 1449–1454.
(36) Petukhova, A.; Paton, A. S.; Gourevich, I.; Kumacheva, E.; Saarinen, J. J.; Sipe, J. E. *Appl. Phys. Lett.* **2006**, *89*, 211908.
(37) Petukhova, A.; Paton, A. S.; Wei, Z.; Gourevich, I.; Nair, S. V.; Ruda, H. E.; Shik, A.; Kumacheva, E. *Adv. Funct. Mater.* **2008**, *18*, 1961–1968.
(38) Takekoh, R.; Li, W.-H.; Burke, N. A. D.; Stöver, H. D. H. *J. Am. Chem. Soc.* **2006**, *128*, 240–244.
(39) Buck, J. R.; Kimble, H. J. *Phys. Rev. A* **2003**, *67*, 033806.
(40) Joannopoulos, J. D.; Meade, R. D.; Winn, J. N. *Photonic Crystals: Molding the Frow of Light*; Princeton University Press: Princeton, 1995.
(41) Helfand, E. *Macromolecules* **1975**, *8*, 552–556.
(42) Matsushita, Y.; Choshi, H.; Fujimoto, T.; Nagasawa, M. *Macromolecules* **1980**, *13*, 1053–1058.
(43) Hashimoto, T.; Shibayama, M.; Kawai, H. *Macromolecules* **1980**, *13*, 1237–1247.
(44) Leibler, L. *Macromolecules* **1980**, *13*, 1602–1617.
(45) Hasegawa, H.; Tanaka, H.; Yamasaki, K.; Hashimoto, T. *Macromolecules* **1987**, *20*, 1651–1662.
(46) Bates, F. S.; Fredrickson, G. H. *Annu. Rev. Phys. Chem.* **1990**, *41*, 525–557.
(47) Mogi, Y.; Kotsuji, H.; Kaneko, Y.; Mori, K.; Matsushita, Y.; Noda, I. *Macromolecules* **1992**, *25*, 5408–5411.
(48) Matsen, M. W.; Schick, M. *Phys. Rev. Lett.* **1994**, *72*, 2660–2663.
(49) Forster, S.; Khandpur, A. K.; Zhao, J.; Bates, F. S.; Hamley, I. W.; Ryan, A. J.; Bras, W. *Macromolecules* **1994**, *27*, 6922–6935.
(50) Khandpur, A. K.; Forster, S.; Bates, F. S.; Hamley, I. W.; Ryan, A. J.; Bras, W.; Almdal, K.; Mortensen, K. *Macromolecules* **1995**, *28*, 8796–8806.
(51) Matsen, M. W.; Bates, F. S. *Macromolecules* **1996**, *29*, 1091–1098.
(52) Hamley, I. W. *The Physics of Block Copolymers*; Oxford University Press: Oxford, UK, 1998.
(53) Bates, F. S.; Fredrickson, G. H. *Phys. Today* **1999**, *52*, 32–38.
(54) Ruzette, A.-v.; Leibler, L. *Nat. Mater.* **2005**, *4*, 19–31.
(55) Okubo, M.; Saito, N.; Takekoh, R.; Kobayashi, H. *Polymer* **2005**, *46*, 1151–1156.
(56) Trent, J. S.; Scheinbeim, J. I.; Couchman, P. R. *Macromolecules* **1983**, *16*, 589–598.
(57) Saito, N.; Takekoh, R.; Nakatsuru, R.; Okubo, M. *Langmuir* **2007**, *23*, 5978–5983.
(58) Helfand, E.; Wasserman, Z. R. *Macromolecules* **1976**, *9*, 879–888.
(59) Semenov, A. N. *Sov. Phys.—JETP* **1985**, *61*, 733.
(60) Ohta, T.; Kawasaki, K. *Macromolecules* **1986**, *19*, 2621–2632.
(61) Matsushita, Y.; Mori, K.; Saguchi, R.; Nakao, Y.; Noda, I.; Nagasawa, M. *Macromolecules* **1990**, *23*, 4313–4316.
(62) Russel, T. P.; Hjelm, R. P.; Seeger, P. A. *Macromolecules* **1990**, *23*, 890–893.
(63) Shull, K. R.; Mayes, A. M.; Russell, T. P. *Macromolecules* **1993**, *26*, 3929–3936.
(64) Xiang, H.; Shin, K.; Kim, T.; Moon, S. I.; McCarthy, T. J.; Russel, T. P. *Macromolecules* **2004**, *37*, 5660–5664.
(65) Ma, M.; Titievsky, K.; Thomas, E. L.; Rutledge, G. C. *Nano Lett.* **2009**, *9*, 1678–1683.
(66) Shibayama, M.; Hashimoto, T.; Hasegawa, H.; Kawai, H. *Macromolecules* **1983**, *16*, 1427–1433.
(67) Saito, N.; Kagari, Y.; Okubo, M. *Langmuir* **2006**, *22*, 9397–9402.
(68) Inoue, T.; Soen, T.; Hashimoto, T.; Kawai, H. *Macromolecules* **1970**, *3*, 87–92.
(69) Hong, K. M.; Noolandi, J. *Macromolecules* **1983**, *16*, 1083–1093.
(70) Roe, R. J.; Zin, W. C. *Macromolecules* **1984**, *17*, 189–194.
(71) Whitmore, M. D.; Noolandi, J. *Macromolecules* **1985**, *18*, 2486–2497.
(72) Mori, K.; Tanaka, H.; Hashimoto, H. *Macromolecules* **1987**, *20*, 381–393.
(73) Tanaka, H.; Hashimoto, T. *Polym. Commun.* **1988**, *29*, 212–216.
(74) Hashimoto, T.; Tanaka, H.; Hasegawa, H. *Macromolecules* **1990**, *23*, 4378–4386.
(75) Tanaka, H.; Hasegawa, H.; Hashimoto, T. *Macromolecules* **1991**, *24*, 240–251.
(76) Winey, K. I.; Thomas, E. L.; Fetters, L. J. *Macromolecules* **1991**, *24*, 6182–6188.
(77) Koizumi, S.; Hasegawa, H.; Hashimoto, T. *Macromolecules* **1994**, *27*, 6532–6540.
(78) Matsen, M. W. *Macromolecules* **1995**, *28*, 5765–5773.
(79) Broseta, D.; Leibler, L.; Joanny, J.-F. *Macromolecules* **1987**, *20*, 1935–1943.
(80) Vanzo, E. *J. Polym. Sci., Part A-1: Polym. Chem.* **1966**, *4*, 1727–1730.
(81) Radford, J. A.; Alfrey, J. T.; Schrenk, W. J. *Polym. Eng. Sci.* **1973**, *13*, 216–221.